

Appendix

Methods

Site and sample collection. Two wastewater treatment plants (WWTPs) serving Montgomery County, Texas were selected for the study. The WWTP186 and WWTP187 serve 65,000 and 70,000 people, respectively (Figure 1). The locations were chosen because Montgomery County recorded a large number of parvovirus infections during the study period based on data from Epic Cosmos (see below). Fifty milliliters of 24-hour composite raw wastewater influent samples were collected using sterile containers by WWTP staff approximately three times per week between 18 December 2023 and 30 August 2024. Samples were sent at 4°C to the laboratory where they were processed immediately. Time between sample collection and receipt at the lab was typically between 1-3 days, during this time, we expect limited degradation of the RNA targets¹. A total of 220 unique samples were processed. At the lab, the wastewater solids were collected from the influent by settling for 10–15 min, and using a serological pipette to aspirate the settled solids into another tube.

Assay specificity and sensitivity testing. We used a previously developed hydrolysis-probe PCR assay for parvovirus B19² (hereafter referred to as “B19V”) that targets the gene for non-structural protein 1 (NS1). To ensure assay specificity and sensitivity, we tested the assay in silico, and in vitro against viruses, bacteria, and synthetic genomes (Table 1). Nucleic-acids were extracted and purified from intact viruses or bacteria as described below for the wastewater solids samples and then used neat as template in droplet digital the 1-step RT-PCR assay. The assay was run in a single well using the cycling conditions and post processing using a droplet reader as described below for the wastewater samples in singleplex. Synthetic parvovirus B19 genomic DNA (ATCC VR-3281SD) was used as a positive control.

For in silico analysis, the primers and probes were first compared to the reference genome (NC_000883.2) from National Center for Biotechnology Information (NCBI) to ensure 100% alignment. After this, genomes from 1 January 2024 to 1 October 2024 were downloaded from NCBI Virus (n=277) and a consensus genome was generated. The assay was then checked against this consensus genome, as well as a subset of individual genomes from the above list. After this, the primers and probes were run through NCBI Blast, excluding Erythroparvovirus primate1 (synonymous with parvovirus B19) and parvovirus B19, to identify potential off-target hits.

Table S1. Viruses used to test specificity are indicated as “non target testing” and viruses used positive controls are indicated as “target testing”. All non-target controls are sold by Zeptomatrix (Buffalo, NY), ATCC (American Type Culture Collection, location), and TWIST (South San Francisco, CA). All the viruses from Zeptomatrix are included in the NATtrol™ Respiratory Verification Panel (Catalog #: NATRSP-BIO).

Virus	Genomic target	Non-target testing (negatives)	Target testing (positives)
Parvovirus B19	Non-structural	Parainfluenza 1 (NATRSP-BIO, Zeptomatrix)	Parvovirus B19

(B19V)	protein 1 (NS1)	Parainfluenza 2 (Zeptomatrix) Parainfluenza 3 (Zeptomatrix) Parainfluenza 4 (Zeptomatrix) Influenza A H1N1pdm (Zeptomatrix) Influenza AH1 (Zeptomatrix) Influenza AH3 (Zeptomatrix) Influenza B (Zeptomatrix) Adenovirus 1 (Zeptomatrix) Adenovirus 3 (Zeptomatrix) Adenovirus 31 (Zeptomatrix) Rhinovirus Type 1A (Zeptomatrix) RSV A (Zeptomatrix) RSV B (Zeptomatrix) SARS-CoV-2 (Zeptomatrix) <i>M. pneumoniae</i> (Zeptomatrix) <i>C. pneumoniae</i> (Zeptomatrix) Metapneumovirus 8 (Zeptomatrix) Coronavirus HKU-1 (Zeptomatrix) Coronavirus 229E (Zeptomatrix) Coronavirus NL63 (Zeptomatrix) Coronavirus OC43 (Zeptomatrix) <i>B. parapertussis</i> (Zeptomatrix) <i>B. pertussis</i> (Zeptomatrix) Synthetic Influenza B RNA (Twist #103003) Synthetic Influenza A H1N1 RNA (Twist #103001) Synthetic Influenza A H3N2 RNA (Twist #103002) Genomic SARS-CoV-2 gRNA (ATCC VR-1986D)	DNA (ATCC VR-3281SD)
--------	-----------------	--	----------------------

40

41 **Solids pre-analytical methods.** Samples were further dewatered by centrifugation, and
42 dewatered solids were suspended in DNA/RNA Shield (Zymo Research, Irvine, CA) at a
43 concentration of 0.75 mg (wet weight)/ml. The DNA/RNA shield was spiked with bovine
44 coronavirus (BCoV) vaccine as a RNA recovery control. This concentration of solids in buffer
45 has been shown to alleviate inhibition in downstream RT-PCR ³. A separate aliquot of
46 dewatered solids was dried in an oven to determine dry weight. RNA was extracted from 6
47 replicate aliquots of dewatered settled solids suspended in the DNA/RNA Shield, and then it
48 was subsequently processed through an inhibitor removal kit . The pre-analytical methods are
49 also provided on protocols.io³.

50

51 **RNA extraction and purification.** RNA extraction and purification was done using the
52 Chemagic Viral DNA/RNA 300 kit H96 for the Perkin Elmer Chemagic 360 (Perkin Elmer,
53 Waltham, MA). It was followed by PCR inhibitor removal with the Zymo OneStep-96 PCR
54 Inhibitor Removal kit (Zymo Research, Irvine, CA). 300 µl of the suspension entered into the
55 nucleic-acid extraction process and 50 µl of nucleic-acids are retrieved after the inhibitor
56 removal kit.

57

58 **Digital droplet RT-PCR analytical methods.** Each replicate RNA extract from each sample (6
59 per sample) was processed to measure human viral nucleic-acid concentrations using digital

60 RT-PCR, each in its own well (6 replicate wells per sample). We quantified the number of copies
61 of B19V DNA using the previously established assay (Table 2). The assay was run in duplex
62 using the probe-mixing approach along with an assay for the SARS-CoV-2 N gene; the probe
63 used to detect B19V was labeled using FAM (6-fluorescein amidite), and the probe used for
64 SARS-CoV-2 was labeled with HEX (hexachlorofluorescein). Extraction negative (BCoV spiked
65 buffer, 2 wells) and positive (buffer spiked with positive control cDNA of SARS-CoV-2 target, 1
66 well) controls, and PCR negative (molecular grade water, 2 wells) and positive controls (cDNA,
67 1 well) were run on each 96 well plate. Nucleic-acids were stored between 2 and 10 months at -
68 80°C prior to these measurements.

69
70 ddRT-PCR was performed on 20 µl samples from a 22 µl reaction volume, prepared using 5.5 µl
71 template, mixed with 5.5 µl of One-Step RT-ddPCR Advanced Kit for Probes (Bio-Rad
72 1863021), 2.2 µl of 200 U/µl Reverse Transcriptase, 1.1 µl of 300 mM dithiothreitol (DTT) and
73 primers and probes mixtures at a final concentration of 900 nM and 250 nM respectively. Primer
74 and probes for assays were purchased from Integrated DNA Technologies (IDT, San Diego,
75 CA) (Table 2. B19V and SARS-CoV-2 nucleic-acids were measured in reactions with undiluted
76 template.

77
78 Droplets were generated using the AutoDG Automated Droplet Generator (Bio-Rad, Hercules,
79 CA). PCR was performed using Mastercycler Pro (Eppendorf, Enfield, CT) with the following
80 cycling conditions: reverse transcription at 50 °C for 60 min, enzyme activation at 95 °C for
81 5 min, 40 cycles of denaturation at 95 °C for 30 s and annealing and extension at 59 °C for 30 s,
82 enzyme deactivation at 98 °C for 10 min then an indefinite hold at 4 °C. The ramp rate for
83 temperature changes were set to 2 °C/second and the final hold at 4 °C was performed for a
84 minimum of 30 min to allow the droplets to stabilize. Droplets were analyzed using the QX200
85 (Bio-Rad). A well had to have over 10,000 droplets for inclusion in the analysis. All liquid
86 transfers were performed using the Agilent Bravo (Agilent Technologies, Santa Clara, CA).

87
88 Thresholding was done using QuantaSoft Analysis Pro Software (Bio-Rad, version 1.0.596) . In
89 order for a sample to be recorded as positive, it had to have at least 3 positive droplets.
90 Replicate wells were merged for analysis of each sample.

91
92 These nucleic-acids were also processed immediately without any storage to measure
93 concentrations of pepper mild mottle virus (PMMoV) RNA, BCoV RNA, and SARS-CoV-2 N
94 gene RNA. PMMoV is highly abundant in wastewater globally⁴ and is used as an internal
95 recovery and fecal strength control⁵. BCoV RNA is used as an exogenous viral nucleic acid
96 recovery control. The measurement of SARS-CoV-2 N gene RNA on fresh, unstored samples
97 can be compared to that measured in the stored samples (described above) as an indication of
98 nucleic-acid degradation during storage and freeze thaw. Details of these measurements, and
99 the measurements themselves, are published in Boehm et al.⁶

100

101
102
103
104
105
106

Table S2. Primer and hydrolysis probes targeting parvovirus B19² (B19V) and SARS-CoV-2 N gene⁷. Each probe contained a fluorescent molecule (FAM for B19V, and HEX for the SARS-CoV-2 N gene), as well as ZEN, a proprietary internal quencher from IDT; and IBFQ, Iowa Black FQ.

Target		Sequence
Parvovirus B19	Forward	CCACTATGAAAACCTGGGCAATA
	Reverse	GCTGCTTTCCTGAGTTCTTCA
	Probe	AATGCAGATGCCCTCCACCCAG
SARS-CoV-2 N gene	Forward	CATTACGTTTGGTGGACCCT
	Reverse	CCTTGCCATGTTGAGTGAGA
	Probe	CGCGATCAAACAACGTCGG

107
108
109
110
111
112
113
114
115

Concentrations of RNA targets were converted to concentrations per dry weight of solids (copies per gram dry weight (cp/g)) using dimensional analysis. The error is reported as standard deviations and includes the errors associated with the Poisson distribution and the variability among the replicates. Three positive droplets across 6 merged wells corresponds to a concentration ~1000 cp/g for solids, respectively). Measured concentrations in the samples are available through the Stanford Digital Repository (<https://doi.org/10.25740/zn011jk5743>).

Parvovirus Case and Symptom Surveillance. Case and syndromic data used in this study came from Epic Cosmos, a dataset created in collaboration with a community of Epic health systems (Epic Cosmos, Epic Systems Corporation, Wisconsin) representing more than 284 million patients from all 50 states, D.C., Lebanon, and Saudi Arabia. Epic Cosmos reflects US population demographics (ref). First, all encounters in the dataset were geographically and temporally filtered to encounters within Montgomery county, Texas between 16 October 2023 and 16 October 16 2024. From this subset, data for parvovirus cases was selected using International Classification of Disease, Tenth Edition (ICD-10) codes B08.3, B34.3 and B97.6 (Erythema infectiosum; Parvovirus infection, unspecified; and Parvovirus as the cause of diseases classified elsewhere).^{8,9} The laboratory testing results for parvovirus were not available through Epic Cosmos; however, prior epidemiological studies have also relied on ICD codes for diagnosis given many children are diagnosed clinically without confirmatory laboratory confirmation. Data was then aggregated at the weekly level and exported as CSV files for

129 analysis. Data are redacted for weeks with fewer than or equal to 10 cases. The date assigned
130 to each week is the last day of the week.

131
132 We also used quarterly data, defined as January through March and every 3 months following,
133 for parvovirus cases as defined above, and hydrops fetalis. Hydrops fetalis diagnosis drew on
134 32 ICD-10 codes encompassing hydrops fetalis due to hemolytic disease, maternal care for
135 hydrops fetalis, and encounter for antenatal screening for hydrops fetalis (ICD-10 P56.*; O36.*;
136 Z36.81) . The data assigned to each quarter represents the last day of the quarter.

137
138 **Statistics.** All data series were not normally distributed based on the Wilks Shapiro test of
139 normality ($p < 0.05$ for case data, B19V, and B19V normalized by PMMoV). Concentrations of
140 B19V and B19V normalized by PMMoV (B19V/PMMoV) were compared between the two
141 WWTPs using Kruskal Wallis tests. We compared the detection of B19V DNA at the two plants
142 using a chi-square test. We tested the hypothesis that weekly median concentrations of B19V
143 and B19V/PMMoV are associated with parvovirus case data using Kendall's tau. Values in the
144 case data < 10 were replaced with 10. We also tested for associations using weekly averages
145 instead of medians. In total, we carried out 11 statistical tests; to account for multiple
146 comparisons, we conservatively used $p = 0.005$ ($0.05/11$) as cut off for $\alpha = 0.05$.

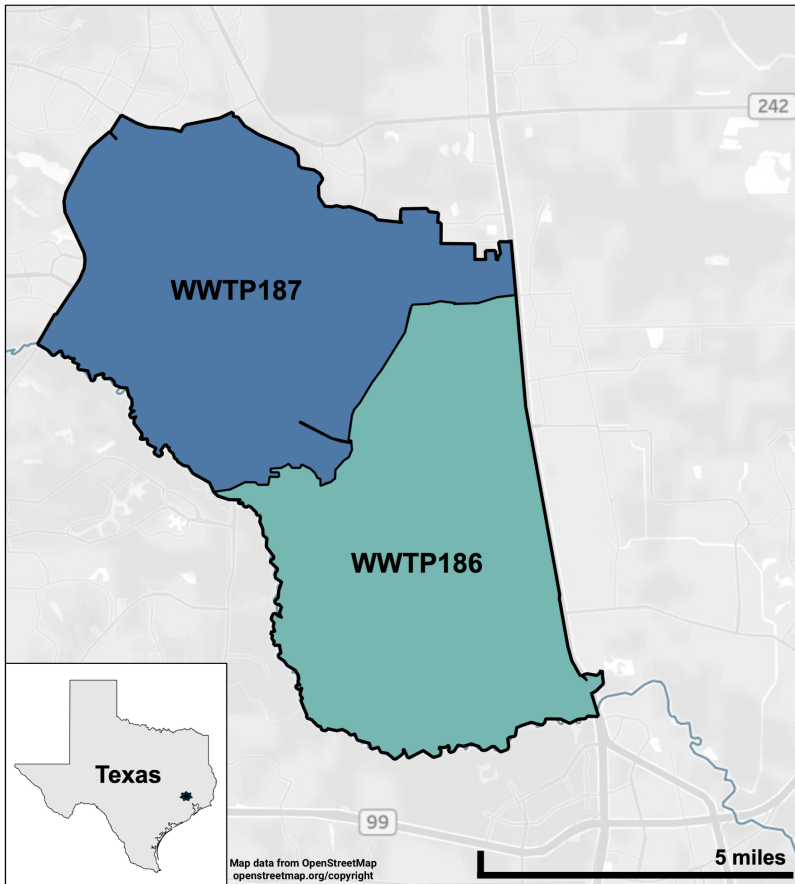
147 148 **Results**

149 **QA/QC.** The previously designed B19V assay was found to be both specific and sensitive, able
150 to detect their intended targets with no cross reactivity. In silico analysis indicated that the assay
151 did not cross react with non-target sequences, and that the assay was able to detect all
152 parvovirus B19. There was no cross reactivity identified in vitro.

153
154 Negative and positive extraction and PCR controls on all plates used for environmental sample
155 testing were negative and positive. Median (interquartile range, IQR) BCoV recoveries were 1.1
156 (0.75, 1.2) for WWTP186 and 0.89 (0.7, 1.1) for WWTP187. Median (IQR) PMMoV were
157 1.9×10^8 ($1.2 \times 10^8 - 2.7 \times 10^8$) cp/g for WWTP186 and 2.2×10^8 ($1.4 \times 10^8 - 3.5 \times 10^8$) cp/g for
158 WWTP187 (Figure 2). BCoV recoveries indicate median recoveries close to 100%, and stable
159 PMMoV between and within WWTPs, respectively. This suggests B19V DNA concentrations
160 can be compared over time and between WWTPs as they have similar high recoveries and
161 consistent fecal strength. Median (IQR) ratio of SARS-CoV-2 N gene concentrations in stored
162 versus fresh samples was 1.5 (1.2, 1.8) at both WWTP suggesting minimal effect of storage.

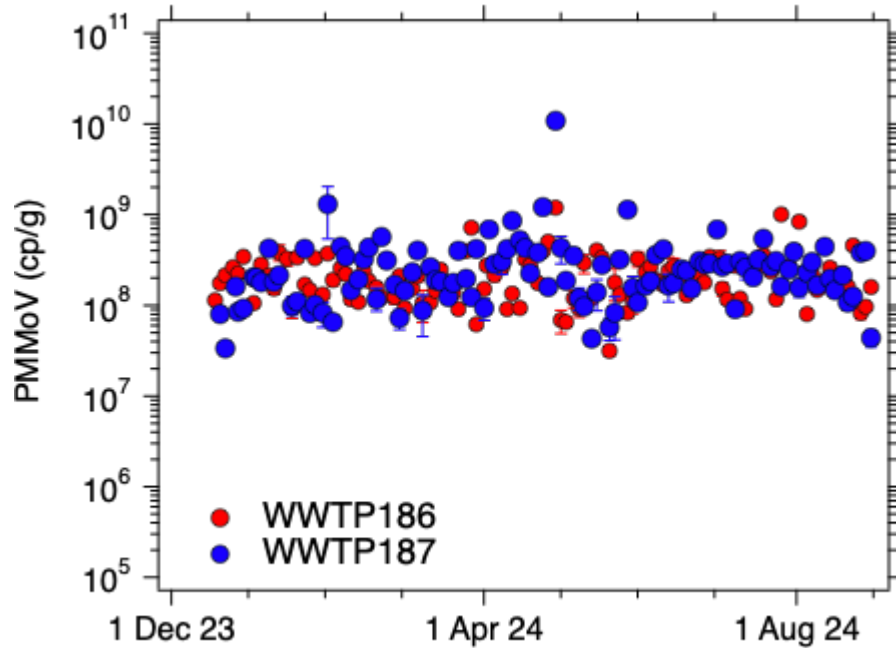
163
164 **Additional details related to the EMMI guidelines.** Across all the samples run in this study
165 ($n=220$), the average (standard deviation) number of partitions (droplets) for the across the 6
166 replicate wells was 89,483 (27,001) for the reaction for duplex B19V and SARS-CoV-2 N gene
167 assays. The volume of the partitions, as reported by the machine vendor is $0.00085 \mu\text{L}$. The
168 mean (standard deviation) of copies per partition for each target was 1.04×10^{-4} (2.37×10^{-4}) and
169 2.57×10^{-3} (3.11×10^{-3}) for B19V and SARS-CoV-2 N gene, respectively. An example fluorescent
170 plot from the QX200 (2 color reader), as well as a spreadsheet version of the EMMI checklist is
171 included in the Stanford Digital Repository with the deposited data
172 (<https://doi.org/10.25740/zn011jk5743>).

173
174
175
176
177
178
179
180
181

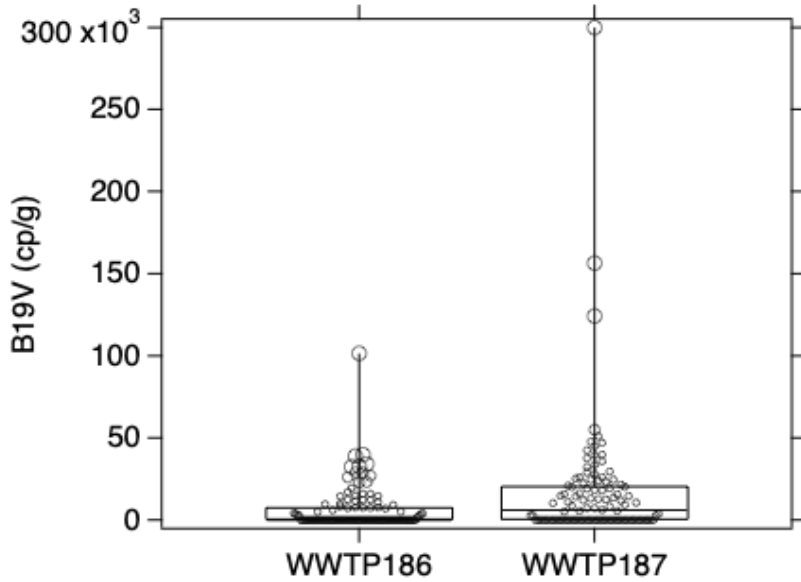


182
183
184
185
186
187
188

Figure S1. Map of the two sewersheds from which wastewater solids were processed in this study. This figure was generated using Tableau; map layer from OpenStreetMap which is open access(openstreetmap.org/copyright).



189
 190 Figure S2. Concentrations of PMMoV measured in the samples, as previously reported⁶. Error
 191 bars represent standard deviations and in some cases are too small to be seen.



192
 193 Figure S3. Box and whisker plot of B19V DNA concentrations at the two WWTPs. Lower,
 194 middle, and upper lines of boxes represent the 25th, 50th (median), and 75th percentiles.
 195 Whiskers extend to minimum and maximum measurements. Data points are shown as circles.

196
 197
 198
 199 (1) Simpson, A.; Topol, A.; White, B.; Wolfe, M. K.; Wigginton, K.; Boehm, A. B. Effect of
 200 Storage Conditions on SARS-CoV-2 RNA Quantification in Wastewater Solids. *PeerJ* **2021**,
 201 9, e11933. <https://doi.org/10.7717/peerj.11933>.

- 202 (2) Toppinen, M.; Norja, P.; Aaltonen, L.-M.; Wessberg, S.; Hedman, L.; Söderlund-Venermo,
203 M.; Hedman, K. A New Quantitative PCR for Human Parvovirus B19 Genotypes. *J. Virol.*
204 *Methods* **2015**, *218*, 40–45. <https://doi.org/10.1016/j.jviromet.2015.03.006>.
- 205 (3) Boehm, A. B.; Wolfe, M. K.; Wigginton, K. R.; Bidwell, A.; White, B. J.; Hughes, B.; Duong;
206 Chan-Herur, V.; Bischel, H. N.; Naughton, C. C. Human Viral Nucleic Acids Concentrations
207 in Wastewater Solids from Central and Coastal California USA. *Sci. Data* **2023**, *10*, 396.
- 208 (4) Symonds, E. M.; Nguyen, K. H.; Harwood, V. J.; Breitbart, M. Pepper Mild Mottle Virus: A
209 Plant Pathogen with a Greater Purpose in (Waste)Water Treatment Development and
210 Public Health Management. *Water Res.* **2018**, *144*, 1–12.
211 <https://doi.org/10.1016/j.watres.2018.06.066>.
- 212 (5) McClary-Gutierrez, J. S.; Aanderud, Z. T.; Al-faliti, M.; Duvallet, C.; Gonzalez, R.; Guzman,
213 J.; Holm, R. H.; Jahne, M. A.; Kantor, R. S.; Katsivelis, P.; Kuhn, K. G.; Langan, L. M.;
214 Mansfeldt, C.; McLellan, S. L.; Mendoza Grijalva, L. M.; Murnane, K. S.; Naughton, C. C.;
215 Packman, A. I.; Paraskevopoulos, S.; Radniecki, T. S.; Roman, F. A.; Shrestha, A.; Stadler,
216 L. B.; Steele, J. A.; Swalla, B. M.; Vikesland, P.; Wartell, B.; Wilusz, C. J.; Wong, J. C. C.;
217 Boehm, A. B.; Halden, R. U.; Bibby, K.; Delgado Vela, J. Standardizing Data Reporting in
218 the Research Community to Enhance the Utility of Open Data for SARS-CoV-2 Wastewater
219 Surveillance. *Environ. Sci. Water Res. Technol.* **2021**, *7* (9), 1545–1551.
220 <https://doi.org/10.1039/D1EW00235J>.
- 221 (6) Boehm, A. B.; Wolfe, M. K.; Bidwell, A. L.; Zulli, A.; Chan-Herur, V.; White, B. J.; Shelden,
222 B.; Duong, D. Human Pathogen Nucleic Acids in Wastewater Solids from 191 Wastewater
223 Treatment Plants in the United States. *Sci. Data* **2024**, *11* (1), 1141.
224 <https://doi.org/10.1038/s41597-024-03969-8>.
- 225 (7) Huisman, J. S.; Scire, J.; Caduff, L.; Fernandez-Cassi, X.; Ganesanandamoorthy, P.; Kull,
226 A.; Scheidegger, A.; Stachler, E.; Boehm, A. B.; Hughes, B.; Knudson, A.; Topol, A.;
227 Wigginton, K. R.; Wolfe, M. K.; Kohn, T.; Ort, C.; Stadler, T.; Julian, T. R. Wastewater-
228 Based Estimation of the Effective Reproductive Number of SARS-CoV-2. *Environ. Health*
229 *Perspect.* **2022**, *130* (5), 057011–1.
- 230 (8) *ICD-10 Version:2019*. <https://icd.who.int/browse10/2019/en> (accessed 2024-12-12).
- 231 (9) *ICD-10 : International Statistical Classification of Diseases and Related Health Problems :*
232 *Tenth Revision, 2004, Spanish version, 1st edition published by PAHO as Publicación*
233 *Científica 544.*